MASTER

PREPRINT UCRL-83463

Lawrence Livermore Laboratory

Calculation of Spin Cutoff Parameters Using Moment Techniques

S. M. Grimes

September 1979

This paper was prepared for presentation at the International Conference on Theory and Applications of Moment Methods in Many Fermion Systems September 10-14, 1979, Ames Iowa

This is a preprint of a paper intended for publication in a journal or proceedings. Since changes may be made before publication, this preprint is made available with the understanding that it will not be cited or reproduced without the permission of the author.

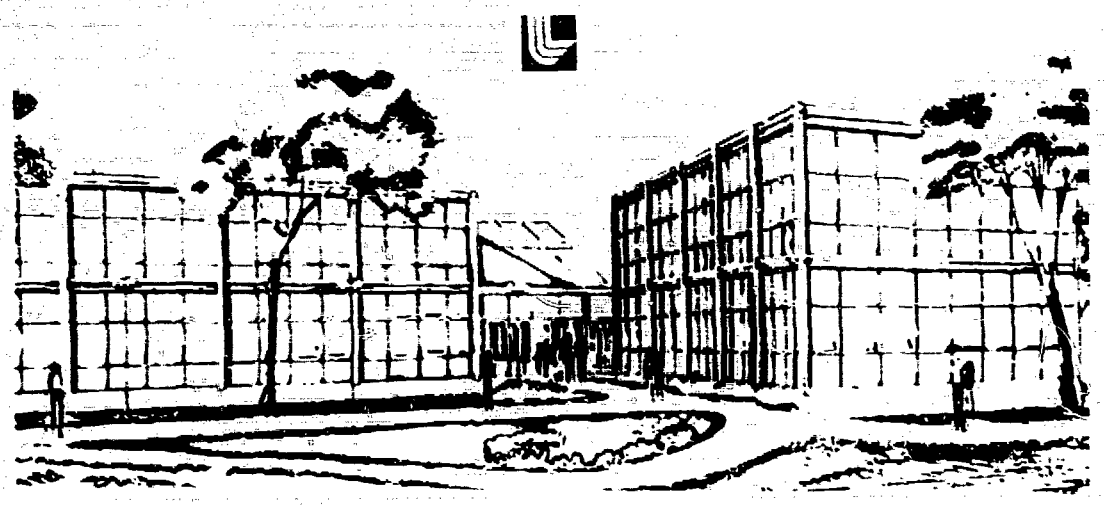

MASTER

DISTRIBUTION OF THIS DOCUMENT IS UNLIMITED

MASTER

CALCULATION OF SPIN CUTOFF PARAMETERS USING MOMENT TECHNIQUES*

S. M. Grimes
Lawrence Livermore Laboratory
University of California
Livermore, California 94550

ABSTRACT

Spectral distribution methods are often applied to the calculation of nuclear level densities. If we require not simply the total number of levels at each energy but also their distribution in spin, we need to know the spin-cutoff parameter and its energy dependence. Recent calculations of the spin-cutoff parameter have shown qualitative agreement with data. Reasons for the remaining discrepancies will be discussed and procedures for improving agreement between theory and experiment will be suggested.

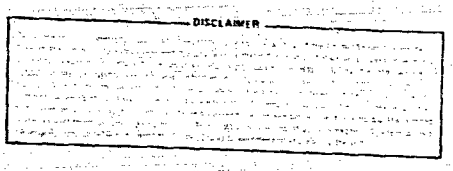

*Work performed under the auspices of the U.S. Department of Energy by the Lawrence Livermore Laboratory under contract number W-7405-ENG-48.

I. INTRODUCTION

Bethe[1] applied the central limit theorem to the distribution of states as a function of angular momentum projection (J_Z) and derived an expression relating the number of levels of spin J at a specific energy to the total number (of all J) at that energy. The fundamental parameter entering this expansion, $\langle J_Z^2 \rangle$, has come to be called the spin-cutoff parameter.

It is usual to define a state as having a specific angular momentum projection on the Z axis and a level as encompassing the (2J+1) degenerate states. Denoting the number of states with angular momentum projection J_Z as $M(J_Z)$, we can express N(J), the number of levels of spin J, as $N(J) = M(J) - M(J+1)$.

This result follows from the fact that every level of spin J has a state with each projection of angular momentum in the range $-J \leq J_Z \leq J$. Thus, M(J) is the number of levels with spin $\geq$ J and M(J+1) is the number with spin $\geq$ J+1. Clearly, the difference between these two is the number of levels of spin J.

Bethe assumed a Gaussian form for M(J), so that

$$M(J) = \frac{N_0}{\sqrt{2\pi}\,\sigma} \exp -J^2/2\sigma^2 \qquad (1)$$

where N_0 is the total number of states and $\sigma (= \langle J_Z^2 \rangle^{\frac{1}{2}})$ is the spin-cutoff parameter. Approximating the difference M(J) - M(J+1) by $\frac{dM}{dJ}\Big|_{J=J+\frac{1}{2}}$, we obtain

$$N(J) = \frac{N_0\ (J+\tfrac{1}{2})}{\sqrt{2\pi}\,\sigma^3}\ \exp\frac{-(J+\tfrac{1}{2})^2}{2\sigma^2} \qquad (2)$$

To generalize this result for a level density as a function of both J and E, one needs to substitute N(E) for N_0 and replace σ with $\sigma(E)$.

If values for N(E) and $\sigma(E)$ are available, one may calculate $\rho(E,J)$ from Eq. (2). Traditionally, both N(E) and $\rho(E,J)$ have been calculated with the thermodynamic approach.[2] This method can easily be programmed for a large computer and does not require large amounts of computer time. It is limited to one-body Hamiltonians, however, and there is at least some indication that the predicted spin-cutoff parameters[3] do not agree well with data. To investigate the extent to which these discrepancies are due to the omission of two-body effects, we must utilize spectral distribution theory.

II. FORMALISM

Use of the formalism of spectral distribution theory allows calculation of level densities and spin cutoff parameters. The method is based on the evaluation of operator traces in a shell model basis. Because of unitarity, these necessarily have the same value as the corresponding traces in the basis of eigenvectors. The values for the traces then allow an expansion for the distribution of eigenvalues as a function of the parameters of interest.

As an example, consider the distribution of states as a function of energy. If the total number of states and the traces of H and H^2 are

known, then we can calculate

$$\langle H \rangle = \frac{\langle\langle H \rangle\rangle}{N} \tag{3}$$

$$\langle H^2 \rangle = \frac{\langle\langle H^2 \rangle\rangle}{N} \tag{4}$$

where $\langle \cdots \rangle$ denotes expectation value, $\langle\langle \rangle\rangle$ denotes trace, and N is the total number of states in the basis. Finally, we have for the distribution of states $\rho(E)$ the form

$$\rho(E) = \frac{N}{\sqrt{2\pi}\,\sigma_H} \exp \frac{-(E - \langle H \rangle)^2}{2\,\sigma_H^2} \tag{5}$$

where $\sigma_H = [\langle H^2 \rangle - \langle H \rangle^2]^{\frac{1}{2}}$.

In a situation where we wish to determine $\rho(E,J)$, two possible expansions are possible, as seen in Fig. 1. Because the early work of Bethe involves first an expansion of the distribution as a function of H and then an expansion in J_Z, this sequence has normally been followed. Some work in spectral distributions has utilized an alternative scheme, in which the J_Z expansion is made first and then H (and H^2) are expanded in powers of J_Z. This yields a Gaussian for each value of J with a separate value of $\langle H \rangle$ and $\langle H^2 \rangle$.

A key question involves the adequacy of two moment expansions. Because most of the trace calculations are carried out with the use of the propagator approach,[4,5] extending the calculations to higher moments has proved to be a difficult task. Until more comparisons between results calculated with only two moments and those including higher moments are available, the need for higher moments will remain uncertain. Such comparisons[6,7] as have been

made, however, support the conclusion that higher moments of H, specifically H^3 and H^4, do improve the agreement between calculation and experiment. Adding powers of J_Z higher than J_Z^2 produces smaller changes.

If we make the usual Bethe expansion (i.e., H first and then J_Z) and postulate that the H distribution is rigorously Gaussian, then higher moments in the J_Z expansion would be included through a Hermite polynomial expansion. More generally, we would allow both distributions to be non-Gaussian in which case the appropriate polynomials for the expansion are the characteristic polynomials[8] defined as

$$\int P_\nu(x)\, P_\mu(x)\, \rho(x)\, dx = \delta_{\mu\nu} \tag{6}$$

where $\rho(x)$ is the level density as a function of the parameter x. Here x would be H if we make the Bethe expansion or J_Z if we project on J_Z first and then H. Note that if $\rho(x)$ is Gaussian, the $P_\nu(x)$ will be Hermite polynomials. Explicit calculation of the $P_\nu(x)$ involves use of traces of order 2ν in the operator x.

III. COMPARISON OF MOMENT EXPANSION RESULTS WITH EXACT DIAGONALIZATION CALCULATIONS

To investigate the importance of higher moments in spectral distribution expansions, it is necessary to study systems where the higher moments as well as the exact energy dependence of the operators of interest are known. Both of these conditions are met in small systems, where the eigenvalues of the system may be obtained from a diagonalization. The eigenvalues, in turn,

may be used to calculate the moments and the exact energy dependence of the operators.

As an example, consider ^{21}Ne in a shell model basis consisting of an ^{16}O core and five valence particles in the $d_{5/2}$, $s_{1/2}$ and $d_{3/2}$ orbitals. This generates 1113 levels (8580 states) of isospin T = 1/2, with spins ranging from 1/2 to 19/2. The two body interaction is that of Chung and Wildenthal.[9]

Fig. 2 shows a Gaussian expansion for the distribution of levels of all spins compared to the exact values. Also indicated is the expansion obtained with terms corresponding to moments as high as H^8. Very small discrepancies are seen for the Gaussian expansion, so the improvement provided by the H^8 expansion is modest.

If the state distribution is projected on the J_Z axis, we obtain the distribution shown in Fig. 3. Again, the Gaussian expansion provides an excellent description of the distribution, with only slight improvement resulting from the inclusion of the J_Z^4 term. Although the size of the basis is small, this provides an impressive justification of Bethe's assumption in treating the J_Z distribution as Gaussian.

Since we are interested in the distribution of levels as a function of both J and E, it is important to check whether the Gaussian distribution is equally appropriate for the levels in a narrow energy range. Results for two typical energy bins are shown in Fig. 4. As in the case of the distribution for the whole basis, the Gaussian fit is quite good.

It therefore appears that in order to expand the level density as a function of E and J, we require the energy dependence of $\langle J_Z^2 \rangle$, with the

energy dependence of $\langle J_Z^4 \rangle$ of lesser interest. Fig. 5 shows the energy dependence of J_Z^2 for the ^{21}Ne system. Values of this parameter calculated from expansions based on the moments of $H^n J_Z^2$ for n = 0,1,2 (second order expansion), for n = 0-4, and for n = 0-8. Clearly, the second order expansion provides a poor fit, particularly in the low energy region which is of most physical interest. Adding terms to produce a fourth order expansion substantially improves the fit and virtually complete convergence occurs for the eighth order fit.

Obtaining the necessary moments for such an expansion is a difficult task. In a situation where the eigenvalues are known, of course, moments of arbitrarily high order can be obtained easily. Since our primary interest for level density calculations is in spaces which are too large for diagonalization, we require alternative means of obtaining the moments. The propagator approach is quite effective for moments as high as $\langle J_Z^2 H^2 \rangle$, but becomes increasingly cumbersome for higher moments. An alternative procedure is the representative vector method.[6] This method is sufficiently new that the only application of it has been to ^{21}Ne, but it is expected to be quite useful in very large spaces. It may also be used[6] in obtaining moments for configurations.

IV. CONFIGURATION EXPANSIONS

The increased difficulty of calculating moments of H higher than H^2 suggests that other possible means of improving the characterization of the energy dependence of operators be investigated. An obvious possibility is

to look at an expansion of the operator of interest in terms of configurations. Even if we restrict our calculations to H and H^2, we can improve our representation of the energy dependence of an operator by evaluating the contributions in terms of a number of Gaussians and summing them up.

For example, instead of calculating $\langle H \rangle$, $\langle HJ_Z^2 \rangle$, $\langle H^2 J_Z^2 \rangle$, $\langle J_Z^2 \rangle$ and $\langle H^2 \rangle$ for the entire basis for ^{21}Ne, we could evaluate these separately for each configuration, defined as a specific number of particles in each shell model orbital. One such configuration, denoted 5 0 0 contains 5 nucleons in the $d_{5/2}$; 0 in the $s_{1/2}$ and 0 in the $d_{3/2}$ orbitals; if all possible arrangements of the five nucleons among the three orbitals are considered, there are a total of 20 such configurations. Each of these will have components distributed among a number of eigenstates, so it is appropriate to define a strength distribution for each configuration. Evaluation of $\langle H \rangle$, $\langle H^2 \rangle$, $\langle J_Z^2 \rangle$, $\langle HJ_Z^2 \rangle$ and $\langle H^2 J_Z^2 \rangle$ for the individual configurations allows the spin cutoff parameter to be expressed as the sum of twenty Gaussians.

Comparison of this calculation with the values from a diagonalization is presented in Fig. 6, taken from Ref. 10. The two moment expansion utilizing configurations is seen to be superior to the two moment expansion for the entire basis and about equal to the four moment expansion for the entire basis. A six moment expansion for the entire basis is closer to the exact values than the configuration expansion.

It may seem puzzling that a twenty Gaussian expansion is not dramatically better, for example, than a four moment expansion in the entire basis. The reason for the modest improvement is that the configuration distributions are highly non-Gaussian.[6] Particularly those configurations which lie either

above or below the centroid of the entire distribution have tails which extend into the central region. This skewing makes the Gaussian assumption particularly poor for configurations, as in seen in Figs. 7 and 8. The entire distribution, on the other hand, is very close to Gaussian. Inclusion of a few additional moments of the Hamiltonian provides excellent convergence for the spin cutoff parameter.

V. SUMMARY

Spectral distribution techniques can yield calculated values for the spin cutoff parameter. The simplest calculations are those which include moments of H no higher than H^2; these apparently provide only a fair representation of the exact values. Better information is obtained from either a configuration expansion or the inclusion of terms corresponding to additional moments of H in the entire basis. Either of these alternatives will mean some increase in complexity of the calculation; a choice between the two approaches will probably be based on convenience and length of the calculation, since either approach can yield accurate values for the spin cutoff parameter.

ACKNOWLEDGEMENTS

The author would like to thank B. A. Pohl for assistance with computer programming and S. D. Bloom and B. J. Dalton for useful discussions.

REFERENCES

1. H. A. Bethe, Phys. Rev. 50, 332 (1936), Rev. Mod. Phys. 9, 69 (1938).
2. J. R. Huizenga and L. G. Moretto, Ann. Rev. Nucl. Sci. 22, 427 (1972).
3. S. M. Grimes, J. D. Anderson, J. W. McClure, B. A. Pohl and C. Wong, Phys. Rev. C10, 2373 (1974).
4. J. N. Ginocchio, Phys. Rev. C8, 139 (1973), S. Ayik and J. N. Ginocchio, Nucl. Phys. A221, 285 (1974).
5. J. B. French and K. F. Ratcliff, Phys. Rev. C3, 94 (1971).
6. S. M. Grimes, S. D. Bloom, R. F. Hausman, Jr., and B. J. Dalton, Phys. Rev. C19, 2378 (1979).
7. F. S. Chang and A. Zucker, Nucl. Phys. A198, 417 (1972).
8. J. P. Draayer, J. B. French and S. S. M. Wong, Ann. Phys. (N.Y.) 106, 472 (1977), 106, 503 (1977).
9. W. Chung and B. H. Wildenthal, private communication; W. Chung, thesis, Michigan State University, 1976 (unpublished).
10. S. M. Grimes, C. H. Poppe, C. Wong, and B. J. Dalton, Phys. Rev. C18, 1100 (1978).

NOTICE

This report was prepared as an account of work sponsored by the United States Government. Neither the United States nor the United States Department of Energy, nor any of their employees, nor any of their contractors, subcontractors, or their employees, makes any warranty, express or implied, or assumes any legal liability or responsibility for the accuracy, completeness or usefulness of any information, apparatus, product or process disclosed, or represents that its use would not infringe privately-owned rights.

Reference to a company or product name does not imply approval or recommendation of the product by the University of California or the U.S. Department of Energy to the exclusion of others that may be suitable.

FIGURE CAPTIONS

Fig. 1: (a & b) Schematic representation of the methods of obtaining level densities as functions of E and J from scalar traces. Figure 1a shows the distribution as a function of E and J. The first projection method is to project on the E axis and calculate $\langle J_Z^2 \rangle^{1/2}$ as a function of E as shown in 1b. An alternative technique is to project first on on the J_Z axis and then express $\langle H \rangle$ and $\langle H^2 \rangle$ as functions of J_Z also shown in 1b. In either case approximate values of $\rho(E,J)$ can be obtained from scalar traces of powers of H and J_Z.

Fig. 2: Distribution of levels with energy for ^{21}Ne calculated in an sd basis with the Chung-Wildenthal[9] interaction. The histogram indicates the exact values (from a diagonalization); the fits are a Gaussian (solid line) and an eighth order expansion (dot-dashed line).

Fig. 3: Distribution of states as a function of J_Z for ^{21}Ne in an sd basis. This encompasses 1113 levels or 8580 states (T = 1/2). The dashed (--) and dot-dashed (·-) lines show J_Z^2 and J_Z^4 expansions, respectively, while the · indicates the exact value.

Fig. 4: Distribution of states as a function of J_Z for ^{21}Ne in an sd basis in two energy bins. The Δ points indicate exact values in the energy bin between -38 and -40 MeV., while the dots indicate the values for the bin between -28 and -30 MeV. Both J_Z^2 and J_Z^4 expansions are shown. The two body matrix elements of Chung and Wildenthal[9] were used in the calculation.

Fig. 5: Energy dependence of the spin cutoff parameter for ^{21}Ne calculated in an sd basis with the Chung-Wildenthal[9] interaction. The points indicate the exact (diagonalization) results and the solid line, dashed line and dot-dashed line denote the second order, fourth order and eighth order expansions, respectively. The sixth order expansion (not shown) is within 2% of the eighth order expansion.

Fig. 6: Same as Fig. 5, except that the expansions are second order in the entire basis (dashed line) and second order in configurations (dot-dashed line). The configuration expansion to second order is almost identical to the whole basis expansion to fourth order (Fig. 5).

Fig. 7: Strength distribution for the 041 configuration (four particles in the $s_{1/2}$ and one in the $d_{3/2}$ orbital) in ^{21}Ne. The histogram shows the exact (diagonalization) results, while the solid line and the dot-dashed line denote Gaussian and eighth-order expansions, respectively. The deviations from a Gaussian form are evident. The interaction used is that of Chung and Wildenthal. This result is from Ref. 6.

Fig. 8: Strength distribution for the 104 configuration (one particle in the $d_{5/2}$ and four in the $d_{3/2}$ orbital) in ^{21}Ne. Shown are Gaussian and eighth order expansions. The non-Gaussian multiple peaking of this distribution is typical of the configurations in this space.

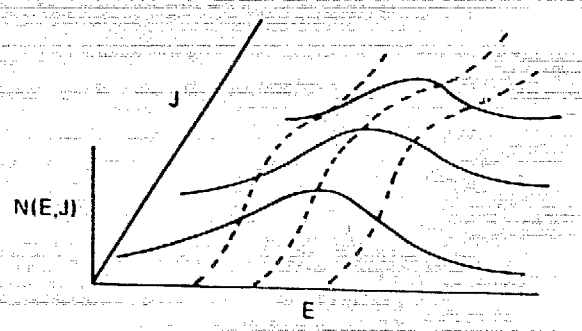

Fig. 1a

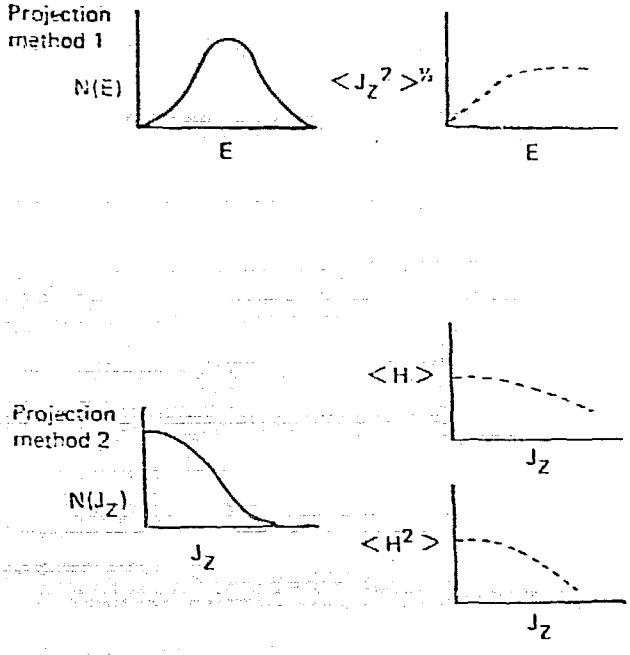
Projection
method 1
N(E)
E
$\langle J_z^2 \rangle^{1/2}$
E
Projection
method 2
$N(J_z)$
J_z
$\langle H \rangle$
J_z
$\langle H^2 \rangle$
J_z

Fig. 1b

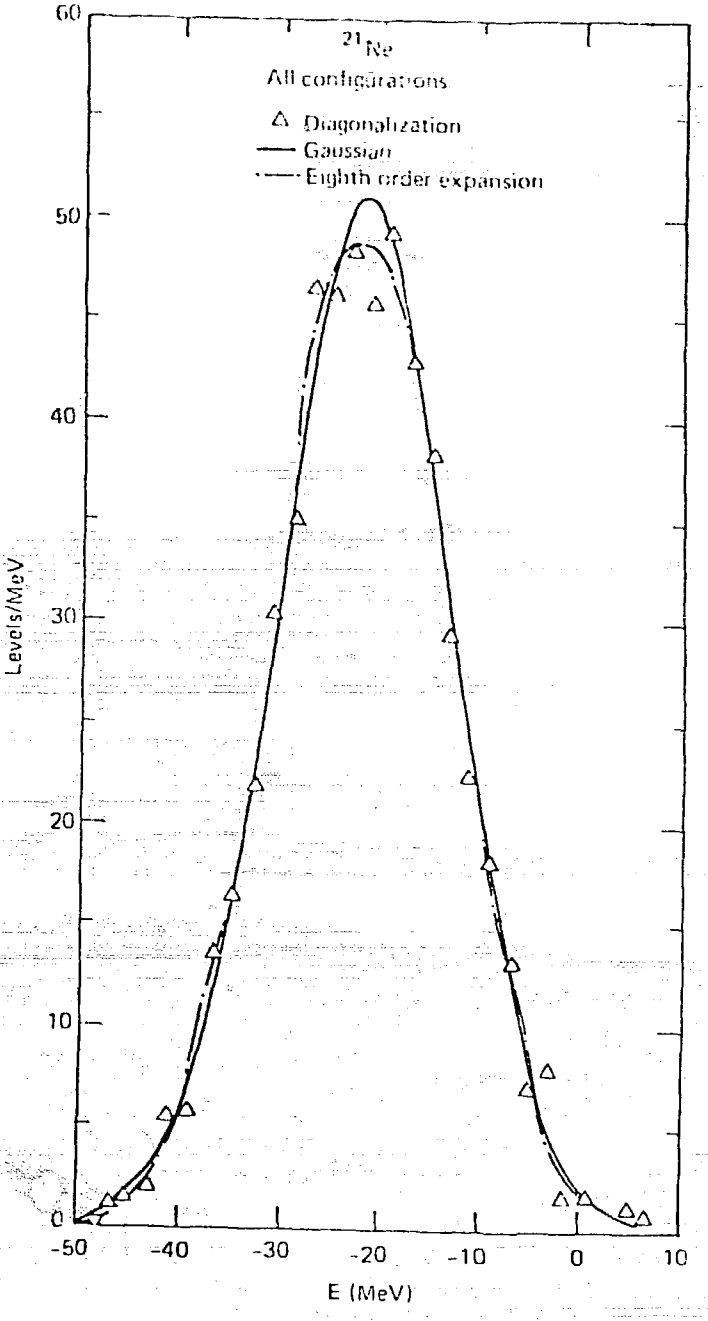
^{21}Ne
All configurations
Diagonalization
Gaussian
Eighth order expansion
Levels/MeV
E (MeV)
60
50
40
30
20
10
0
-50
-40
-30
-20
-10
0
10

Fig. 2

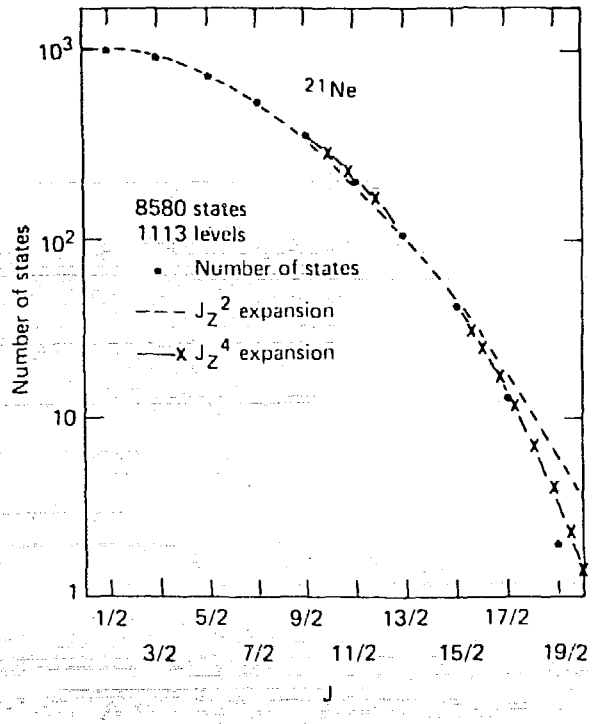
10^3
10^2
10
1
Number of states
^{21}Ne
8580 states
1113 levels
Number of states
J_z^2 expansion
J_z^4 expansion
1/2
3/2
5/2
7/2
9/2
11/2
13/2
15/2
17/2
19/2
J

Fig. 3

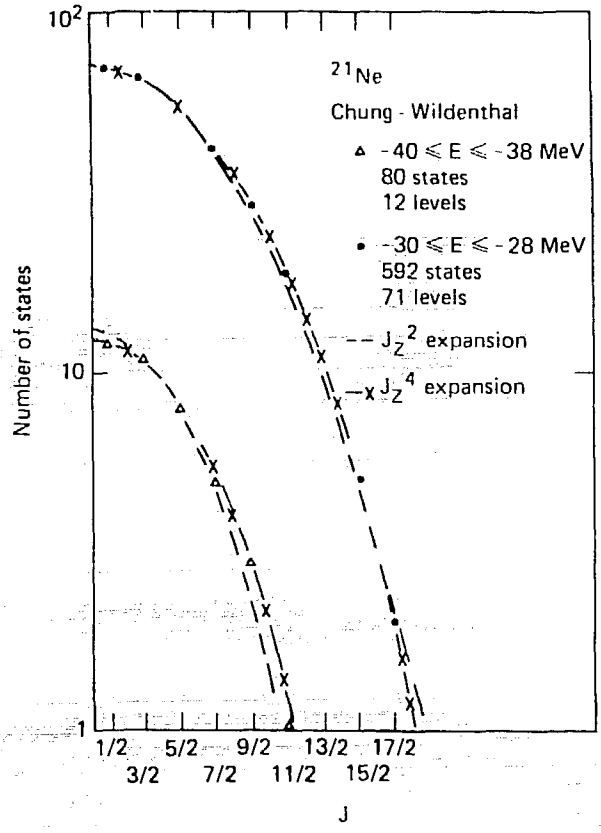
10^2
10
1
Number of states
^{21}Ne
Chung - Wildenthal
△ -40 ⩽ E ⩽ -38 MeV
80 states
12 levels
• -30 ⩽ E ⩽ -28 MeV
592 states
71 levels
-- J_z^2 expansion
—x J_z^4 expansion
1/2 3/2 5/2 7/2 9/2 11/2 13/2 15/2 17/2
J

Fig. 4

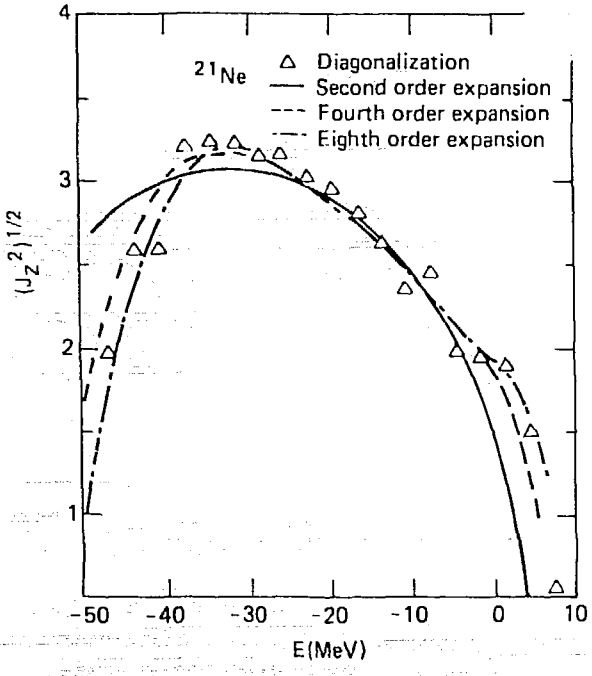
^{21}Ne
Diagonalization
Second order expansion
Fourth order expansion
Eighth order expansion
$(J_z^2)^{1/2}$
E(MeV)
4
3
2
1
-50
-40
-30
-20
-10
0
10

Fig. 5

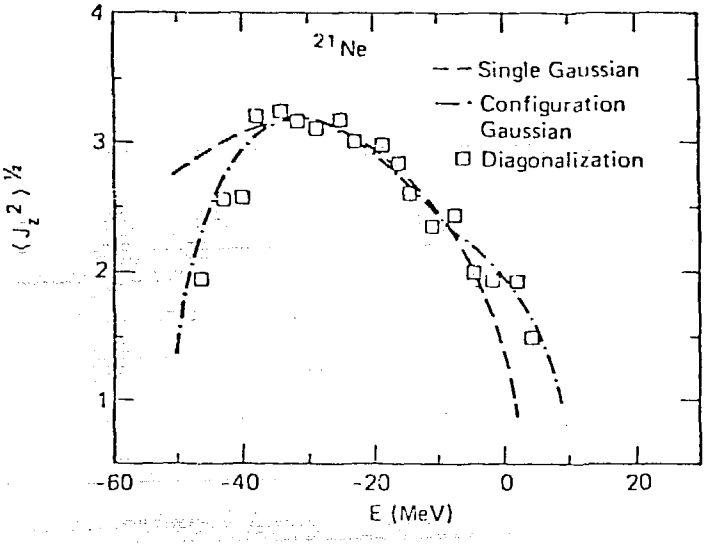
^{21}Ne
Single Gaussian
Configuration Gaussian
Diagonalization
$\langle J_z^2 \rangle^{1/2}$
4
3
2
1
-60
-40
-20
0
20
E (MeV)

Fig. 6

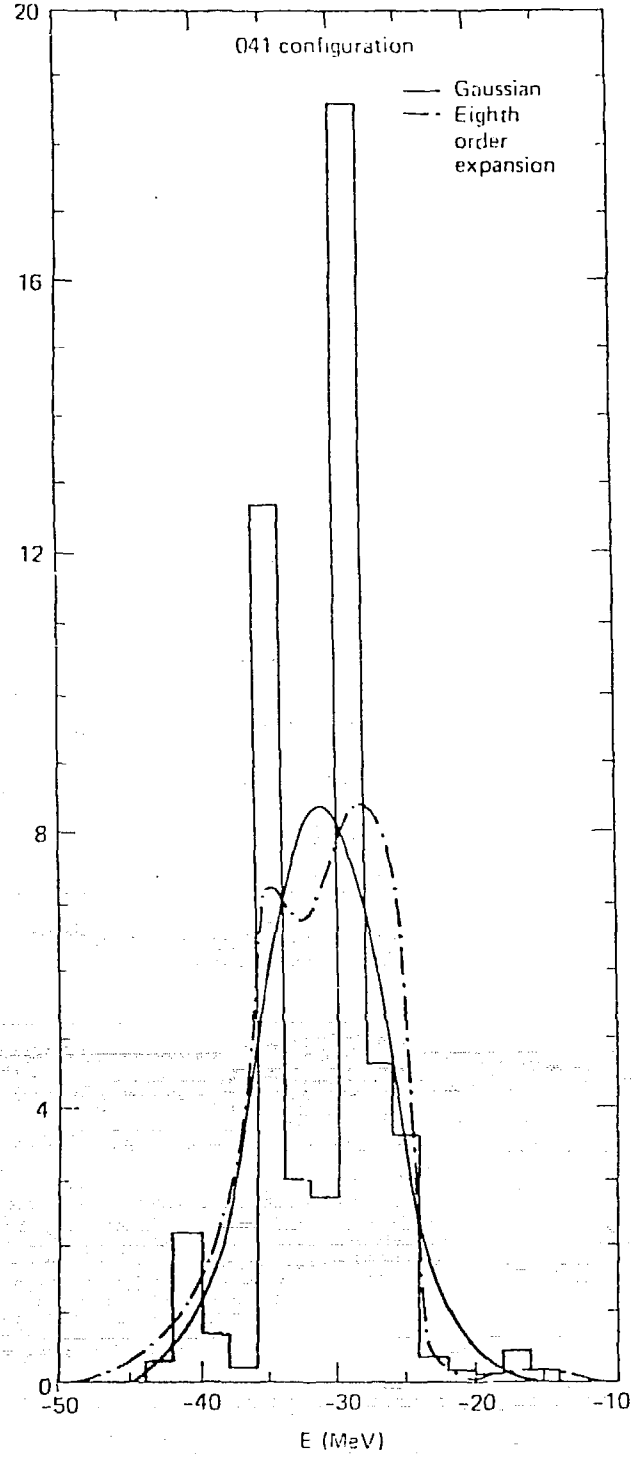
041 configuration
Gaussian
Eighth order expansion
20
16
12
8
4
0
-50
-40
-30
-20
-10
E (MeV)

Fig. 7

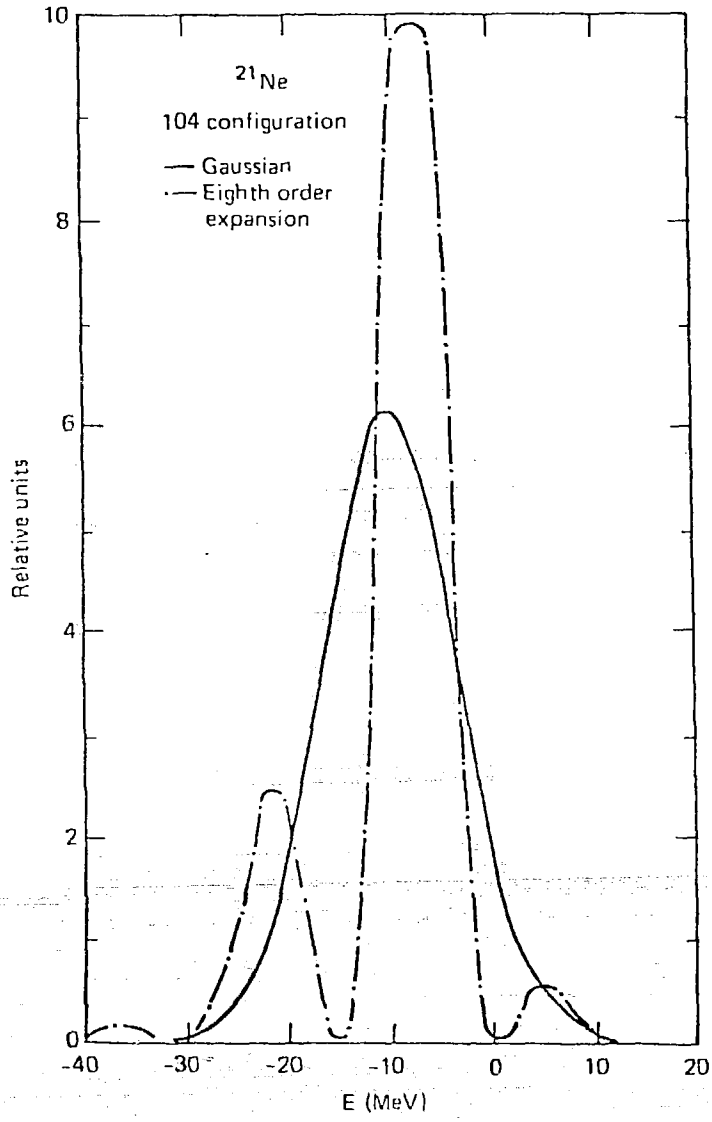
^{21}Ne
104 configuration
Gaussian
Eighth order expansion
Relative units
E (MeV)
10
8
6
4
2
0
-40
-30
-20
-10
0
10
20

Fig. 8